Analog simulation of underdamped stochastic systems driven by colored noise: Spectral densities

F. Marchesoni, E. Menichella-Saetta, M. Pochini, and S. Santucci
Dipartimento di Fisica, Università degli Studi di Perugia, via Elce di Sotto, I-06100 Perugia, Italy
(Received 7 October 1987)

Stochastic relaxation in underdamped nonlinear potentials driven by exponentially time-correlated noise is studied thoroughly by means of analog simulation. The experimental data reported herein should help to tie down future theoretical investigations. A novel dependence of the observed quantities on the noise correlation time τ is revealed: all of the quantities measured are a function of τ^2. In particular, the escape rate in a quartic double-well potential decreases exponentially with increasing τ^2. The relevant spatial spectral densities are also determined for both the monostable and the bistable quartic potential on varying τ. Previous theoretical predictions for the white-noise ($\tau=0$) limit are thus checked. The frequency of the resonance peak is shown to shift depending on τ^2. Finally, some effort has been paid at justifying theoretically the results obtained.

I. INTRODUCTION

The theory of stochastic processes has been successful in modeling a variety of physical phenomena in statistical mechanics, chemical physics, and microelectronics.[1-3] Most models comprise one or more dynamical variables driven by mechanical (nonlinear) forces and subject to external fluctuations, the statistics of which has to be determined. The random variables describe the subsystem of interest; its interaction with the external environment, assumed at equilibrium (thermal bath), is separated into a deterministic and a stochastic coupling. For the splitting of the whole system into a subsystem of interest and a thermal bath being realistic, the fluctuations accounted for in the model ought to be represented by non-Markovian (colored or time-correlated) random variables. Moreover, the very same interaction with the thermal bath provides for the damping (or dissipation) mechanism, which in turn ensures the existence of a stationary state for the model stochastic process.

The study of nonlinear stochastic systems driven by colored noise has been undertaken by a number of investigators.[3-10] It must be said that in spite of much effort no conclusive theory has been elaborated that reproduces the relevant features of such a problem. For the sake of simplicity most authors addressed the limit of large damping (overdamped limit), where perturbation expansions in the noise parameters (intensity and correlation time) may be formally worked out.[3-5] Perturbation schemes, whatever the generating technique, are not applicable to non-Markovian processes, because in most cases they result in intractable asymptotic expansions.[6-10] Up to now, reliable solutions to non-Markovian stochastic differential equations (SDE) are only obtainable by means of numerical algorithms.[2,10,11] An alternative approach to this class of stochastic processes is provided by both analog[12] and digital simulation.[6,13] In conclusion, we can confirm that nonlinear stochastic systems in the overdamped limit have been characterized satisfactorily, even if a comprehensive theoretical treatment is still missing.

In the limit of vanishingly small damping (underdamped limit), instead, much work has to be done. After Kramers's pioneering paper[14] not much attention was paid to the problem of stochastic relaxation in the limit of zero damping. Only in recent years has new interest been conveyed to the question of the escape rate in underdamped bistable potentials—the results of theoretical, numerical, and digital simulation studies are reported in Refs. 15-17. Perturbation expansions are known to work for weakly anharmonic monostable potentials.[18,19] In all of these investigations, however, the external fluctuation is assumed to be Markovian (white or time delta correlated). No attempt has been made at incorporating the effect of colored noise, because of the discouraging difficulties encountered. Indeed, the convergence of the numerical algorithms of Refs. 2 and 11 (continued fraction expansions) for underdamped non-Markovian processes is poor, since the minimal set of variables is too large to treat. Moreover, digital simulation produces results with far too low statistics to be reliable. Even the most sophisticated digital simulation technique expounded in Ref. 13 cannot be applied in the presence of colored noise due to the lack of an explicit expression (not even numerical) for the stationary probability distribution function.

In spite of these difficulties, stochastic relaxation of underdamped nonlinear systems is an unavoidable problem to deal with in many areas of statistical mechanics and applied physics.[1-3] In the present paper we attack the problem by means of analog simulation. It is our purpose to present a comprehensive collection of experimental results for both bistable and monostable systems which should provide a clue to the theory of non-Markovian processes. The accuracy of our analog simulation has been assessed by comparison with the existing predictions for the white-noise limit. We believe that, at the present stage of our knowledge, analog simulation is the most reliable tool for tackling this problem.

The paper is organized as follows. In Sec. II we introduce the study model we chose for our simulations. One-dimensional Brownian motion is studied in both a

monostable (Duffing oscillator) and a bistable (quartic double-well) potential driven by an *exponentially* time-correlated noise. Details on the analog simulator are reported in the Appendix. Sections III and IV are devoted to the presentation and the discussion of our results for the bistable potential. The spatial autocorrelation function and the relevant spectral density are determined in Sec. III for several values of the damping constant and the noise correlation time. An exponential decrease of the escape rate with the square of the noise correlation time is observed and discussed in Sec. IV. The spatial autocorrelation function and spectral density of Brownian motion in the monostable potential are reported in Sec. V. General properties of the dependence of the quantities studied on the noise correlation time are evidentiated and interpreted theoretically in Sec. VI.

II. THE MODEL

The stochastic process simulated in our investigation obeys the following SDE for Brownian motion:

$$\ddot{x} = -\gamma\dot{x} - V'(x) + \epsilon(t) , \tag{2.1}$$

where $V(x)$ is a nonlinear potential and $\epsilon(t)$ an external Gaussian noise. In the white-noise limit the following correlation functions provide a complete description of the noise statistics:

$$\langle \epsilon(t) \rangle = 0, \quad C_\epsilon(t) = \langle \epsilon(t)\epsilon(0) \rangle = 2\gamma kT\delta(t) . \tag{2.2}$$

The fluctuation-dissipation relationship here is understood.

The anharmonic potential simulated has the symmetric form

$$V(x) = \tfrac{1}{4}b\left[x^2 - \frac{a}{b}\right]^2 , \tag{2.3}$$

with $b > 0$. For $a < 0$, the potential $V(x)$ represents a monostable quartic potential which we agree to term Duffing oscillator (DO) potential. For $a > 0$, the potential $V(x)$ is bistable with minima located at $x_\pm = \pm\sqrt{a/b}$ and potential barrier height $\Delta V = a^2/4b$. The characteristic frequencies of this choice of the function $V(x)$ are given by the square root of its curvature about the well bottom $V''(x_\pm) = 2a$ and the barrier top $|V''(0)| = a$. This is the well-known quartic double-well (QDW) potential.

Our noise generator[20] produces a random signal which is Gaussian to a good approximation and correlated in time (i.e., colored). The actual correlation functions for the generated noise are

$$\begin{aligned} &\langle \epsilon(t) \rangle = 0 , \\ &C_\epsilon(t) = \langle \epsilon(t)\epsilon(0) \rangle = (kT\gamma/\tau)e^{-|t|/\tau} . \end{aligned} \tag{2.4}$$

$\epsilon(t)$ is exponentially time correlated with correlation time τ.

The non-Markovian SDE (2.1) and (2.4) is equivalent to the three-dimensional Markovian system (Doob's theorem[1-3])

$$\begin{aligned} &\dot{x} = v, \quad \dot{v} = -\gamma v - V'(x) + \epsilon , \\ &\dot{\epsilon} = -\epsilon/\tau + \eta(t)/\tau , \end{aligned} \tag{2.5}$$

where $\eta(t)$ is a Gaussian external noise with correlation functions given by Eq. (2.2). We refer to this system of equations as to the system of SDE's simulated by our analog circuit (see the Appendix).

Our system is characterized by three time scales: the noise time correlation τ, the damping relaxation time γ^{-1}, and the librational period $T_p = \nu_p^{-1}$ of the Brownian particle with coordinate $x(t)$ about the potential minima. The frequency ν_p depends on the potential and noise parameters. It has been proved (see, e.g., Ref. 20) that for vanishingly small damping constant γ the spatial fluctuation increases greatly. As a consequence, the effect of nonlinearity on the resonance frequency ν_p is important. Unfortunately, ν_p cannot be determined analytically, and therefore the damping condition of the system can only be determined empirically. The spatial spectral density shows no resonance peak in the overdamped limit $\gamma \gg \omega_p$ (with $\omega_p \equiv 2\pi\nu_p$). With decreasing γ a resonance peak shows up at about a certain frequency ν_p. The underdamped limit corresponds to the requirement $\gamma \ll \omega_p$.

The noise correlation time simulated in our experiment is short compared to T_p, i.e., $\omega_p\tau \lesssim 1$, and negligible compared to γ^{-1}. One would expect that our results might be interpreted in terms of a suitable τ expansion of the type introduced in Ref. 16. In fact, at $\tau = 0$ both the DO and the QDW potential have been investigated in some detail. In particular, in Refs. 15–17 the escape rate in an underdamped bistable potential driven by white noise was determined analytically at low temperature ($kT \ll \Delta V$). The spatial spectral densities for the DO potential, too, have been obtained at low temperature or, equivalently, for weak nonlinearity.[18,19] Of course, it would be desirable to incorporate explicitly the colored-noise effects in the analytical approaches of Refs. 16 and 18. This is matter for ongoing work. In the following sections we limit ourselves to presenting some experimental results which are expected to help to tie down future theoretical predictions.

III. SPATIAL RELAXATION IN A BISTABLE POTENTIAL

Let us start our investigation with the more complicated case of the QDW potential. In the limit of low temperature or, equivalently, high-potential barrier, it is possible to distinguish between two important mechanisms:[21] the relaxation towards a quasistationary state inside a single potential well and the escape process of the Brownian particle over the potential barrier. The latter is by far the slowest process taking place in a bistable potential at low temperature. In the present section we shall concentrate on some general properties of the spatial relaxation in a bistable potential driven by colored noise.

The operating conditions of our analog simulator have been chosen as follows.

(a) *High potential barriers.* Our results refer to barrier height ΔV to thermal kT ratios ranging between 1 and 3.

In most cases the potential parameters are fixed: $a=0.38\times10^{8}\ \mathrm{s}^{-2}$ and $b=0.96\times10^{6}\ \mathrm{s}^{-2}$ (x is given in dimensionless units). The coefficient of the linear term a has been changed to $a=0.27\times10^{8}\ \mathrm{s}^{-2}$ in some measurements reported in Fig. 6.

(b) *Low viscosity.* The damping constant γ can be tuned within the interval $(0.04/0.01)[V''(x_{\pm})]^{1/2}$, where the underdamped limit properties of Brownian motion are clearly distinguishable.[14–17] In particular, we have checked that in such a regime the rate of escape (see Sec. IV) depends linearly on γ.

(c) *Small- (to intermediate-) noise correlation time.* With our processing system (see the Appendix) accurate measurements of the long-time features of the spatial autocorrelation function (ACF), e.g., the rate of escape, have been obtained for values of τ up to about the characteristic librational period inside a potential well $\omega_p\tau\lesssim1$. Moreover, due to the low-viscosity condition (b), the noise correlation time τ is much shorter than the reciprocal of the damping constant, i.e., $\gamma\tau\ll1$.

The steady-state relaxation dynamics of a bistable system can be characterized by means of the normalized equilibrium ACF

$$C(t)=\langle x(t)x(0)\rangle/\langle x^{2}\rangle\ . \tag{3.1}$$

In our experiment $C(t)$ is measured by taking the ACF over a sample of 512 points of the discretized output signal $x(t)$ and then averaging over up to 10^{4} samples. Such a procedure turned out to be fast and very accurate.[20]

$C(t)$ has been determined for several circuital configurations. A few examples are reported in Fig. 1. $C(t)$ decays exponentially for finite values of τ and γ. A superimposed damped oscillation shows up to τ and/or γ tending to zero. Unfortunately, the performances of our apparatus did not permit us to explore the limit when γ and τ vanish. An analytical study of such a limit is presented in Ref. 16.

The nonoscillating decay of $C(t)$ allows us to determine uniquely the smallest decay rate $\lambda(\tau)$ for the spatial relaxation. $\lambda(\tau)$ is measured by taking the natural logarithm of the exponential decay tail of $C(t)$. Our results for $\lambda(\tau)$ are given with an estimated error of less than 10% (Sec. IV).

A quantitative analysis of the spatial ACF can be carried out by introducing the power spectrum of the output signal

$$S(\omega)=\kappa\,|\,x(\omega)\,|^{2}\ . \tag{3.2}$$

The constant κ is chosen in order to normalize $S(\omega)$ to unit

$$\int_{0}^{\infty}S(\omega)d\omega=1\ . \tag{3.3}$$

In view of the Wigner-Khintchine theorem,[2] $S(\omega)$ coincides with the cosine-Fourier transform of $C(t)$.

Our results for $S(\omega)$ are reported in Figs. 2–4 for different values of $\Delta V/kT$, τ, and γ. In Fig. 2 we have simulated the potential parameters adopted by Voigtlaender and Risken in Fig. 9 of Ref. 16: $\Delta V/kT=1$, $\gamma=0.1\sqrt{a}$, and ω is expressed in units of $\sqrt{a}$. We see that with decreasing τ the experimental curves approach the corresponding numerical predictions of Ref. 16 for the white-noise limit. The accuracy of our simulation looks rather good.

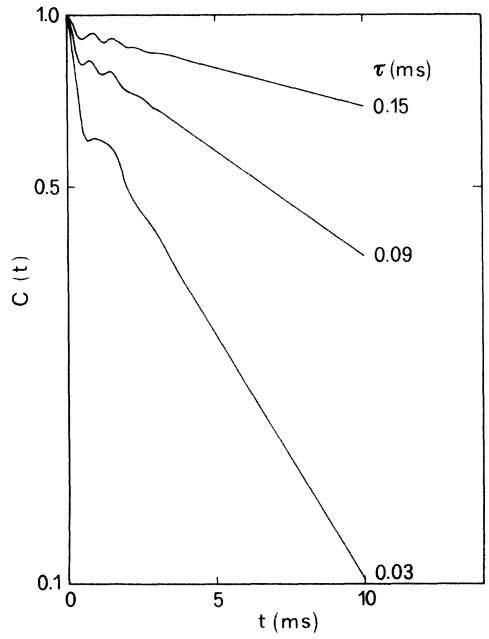

FIG. 1. $C(t)$ for the QDW potential at different values of τ. Relevant parameter values: $\Delta V/kT=2$, $\gamma=0.06\sqrt{2a}$. a and b are given in Sec. II.

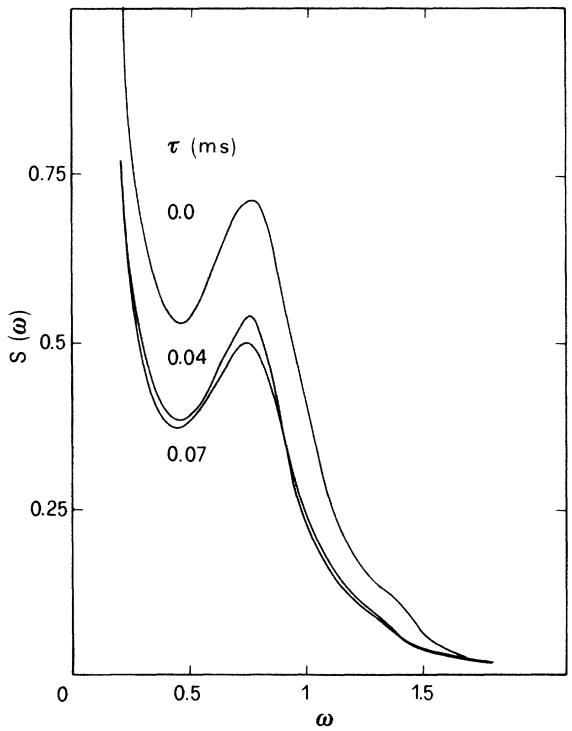

FIG. 2. $S(\omega)$ for the QDW potential. The curve for $\tau=0$ is the numerical prediction of Ref. 16. The curves with finite τ are the result of analog simulation. Relevant parameter values: $\Delta V/kT=2$, $\gamma=0.07\sqrt{2a}$. ω is given in units of $\sqrt{a}$.

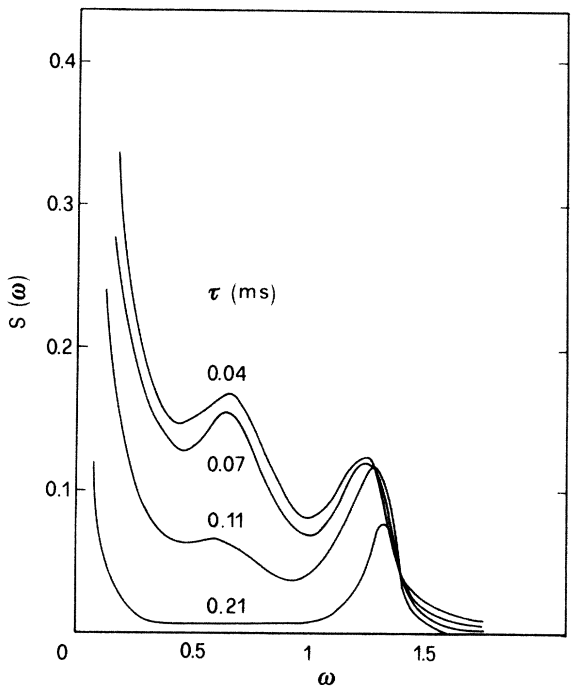

FIG. 3. $S(\omega)$ for the QDW potential at different values of τ. Relevant parameter values: $\Delta V/kT=2$, $\gamma=0.06\sqrt{2a}$. ω is given in units of $\sqrt{a}$.

The general features of $S(\omega)$ may be summarized as follows.

(i) At small frequencies $S(\omega)$ seems to decay with the power law $S(\omega)\approx\omega^{-2}$. In fact, our data for $S(\omega)$ are better fitted by a Lorentzian line (see Sec. IV).

(ii) For high-potential barriers—in Figs. 3 and 4, $\Delta V/kT=2$—$S(\omega)$ exhibits two peaks at about $\omega\approx\sqrt{2a}$ and $\sqrt{a/2}$, respectively. As explained in Ref. 16 the maximum at half the characteristic frequency $[V''(x_{\pm})]^{1/2}$ stems from those particles that have been activated to energies larger than ΔV and thus oscillate from the left to the right potential well and vice versa (activation peak). The maximum at $\omega\approx[V''(x_{\pm})]^{1/2}$ stems from those particles that have energy less than ΔV and, therefore, oscillate inside a single well (libration peak). Note that at higher temperature the former peak is enhanced with respect to the latter one. That is consistent with the above explanation.[16]

(iii) The peak structure of $S(\omega)$ is enhanced with decreasing γ and τ—compare Figs. 3 and 4. Most notably, the activation peak flattens out compared to the librational peak for long-noise correlation time. It is conceivable that such a behavior affects the escape mechanism in the presence of colored noise to an extent which is to be determined yet.

The frequency separation between the region of power-law decay and the activation-libration peak structure is clear cut at low temperature (Figs. 3 and 4). This corresponds to the separation between the escape mechanism and the relaxation process inside the potential wells we assumed in the first place.

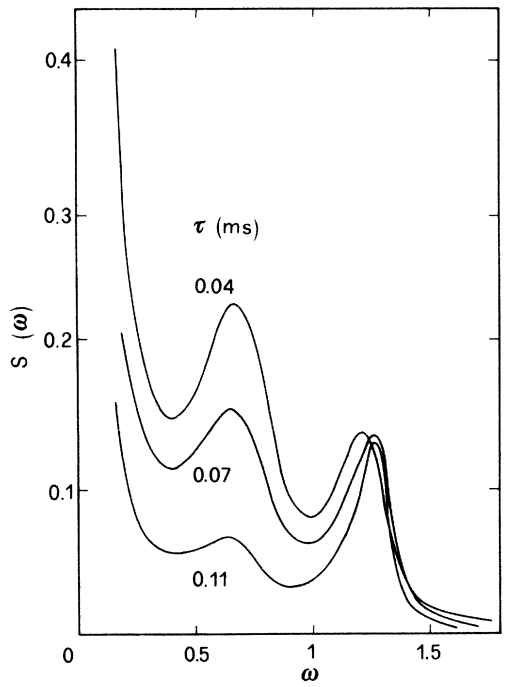

FIG. 4. As in Fig. 3 but for $\gamma=0.04\sqrt{2a}$.

IV. ESCAPE RATE DRIVEN BY COLORED NOISE

Let us focus now on the low-frequency behavior of $S(\omega)$. A closer inspection of the experimental results shows that at low frequencies the power spectrum of $x(t)$ can be approximated by the Lorentzian curve [see Eq. (3.2)]

$$|\hat{x}(\omega)|^2=A\frac{\lambda}{\lambda^2+\omega^2}\ , \tag{4.1}$$

where λ is the smallest nonvanishing eigenvalue of the Fokker-Planck equation associated with the problem (2.5) and must be related to the rate of the escape process out of the potential barrier.[16]

A is smaller than the expectation value $\langle x^2\rangle$ and approaches $\langle x^2\rangle$ at low temperatures,[16] i.e., $A\approx(a/b)(1-kT/4\Delta V)$. To a first approximation $(kT\ll\Delta V)$

$$S(0)\approx 1/\lambda(\tau)\ . \tag{4.2}$$

In Fig. 5 the behavior of $S(\omega)$ at small frequencies is displayed for the circuital configuration of Fig. 3. For large values of τ the maximum of $S(\omega)$ in $\omega=0$ is enhanced. This implies that the smallest eigenvalue $\lambda(\tau)$ decreases with increasing τ. An ω^{-2} fall off of $S(\omega)$ is clearly distinguishable at frequencies much larger than $[V''(x_{\pm})]^{1/2}$ and, therefore, more apparent for large values of τ. Such a behavior was detected first by the authors of Ref. 22.

Our notation for $\lambda(\tau)$ is purposely ambiguous. In Sec. III $\lambda(\tau)$ denotes the smallest decay rate of $C(t)$. Here, instead, $\lambda(\tau)$ is the smallest eigenvalue of the Fokker-Planck equation related to the system of SDE's under study. Finally, we often refer to $\lambda(\tau)$ as to the escape rate in the relevant bistable potential. As a matter of fact, the

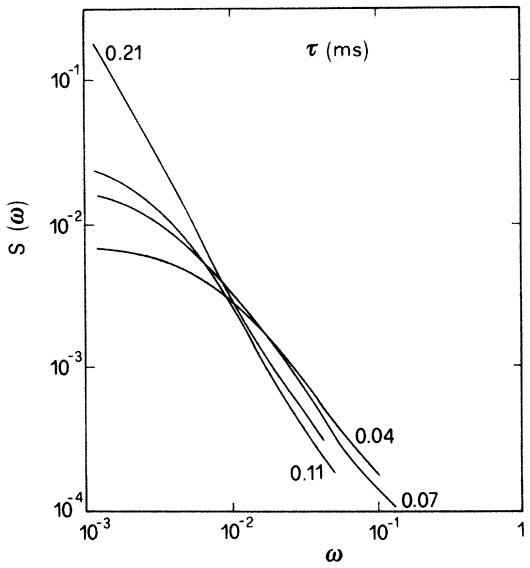

FIG. 5. $S(\omega)$ vs ω at low frequencies for the same circuit configuration as in Fig. 3.

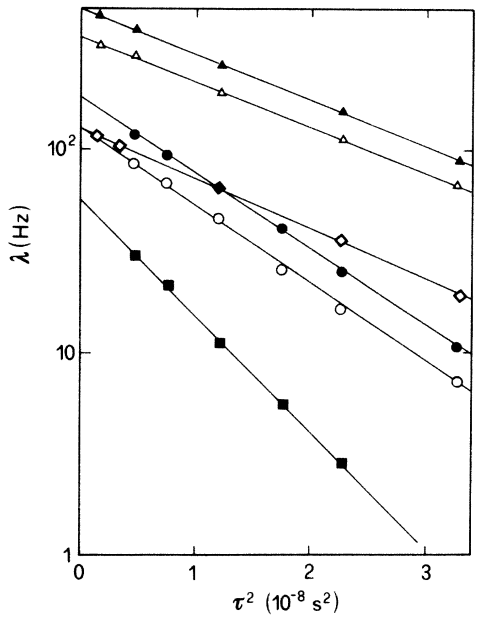

FIG. 6. Plot of $\lambda(\tau)$ vs τ^2 in two underdamped configurations $\gamma=0.06\sqrt{2a}$ (open dots) and $\gamma=0.08\sqrt{2a}$ (closed dots) and different values of the temperature $\Delta V/kT=1$ (triangles), $\Delta V/kT=2$ (squares and rhombi), and $\Delta V/kT=3$ (circles). All measurements have been carried out with $a=0.38\times10^8$ s^{-2} but for the set of rhombi $a=0.27\times10^8$ s^{-2}. The best exponential fit for each set of dot is also displayed.

smallest Fokker-Planck eigenvalue and the smallest $C(t)$ decay rate do coincide by definition.[1] The usual definition[3] of rate of escape may look inadequate for the three-dimensional problem (2.5).[10] However, also in view of the properties of $C(t)$ illustrated in Sec. III, the close correspondence between $\lambda(\tau)$ and the rate of escape can be assessed at low temperature.[16] Anyway, throughout the present work $\lambda(\tau)$ has been measured as the smallest decay rate of $C(t)$.

In order to verify the prediction (4.2), we measured $\lambda(\tau)$ for a wide range of parameter values.[23] The main properties of $\lambda(\tau)$ thus detected can be summarized as follows (Fig. 6).

(i) $\lambda(\tau)$ decreases exponentially with increasing τ^2 according to the heuristic law

$$\lambda(\tau)=\lambda(0)e^{-\kappa_0\tau^2}. \tag{4.3}$$

Such a behavior has been checked down to the smallest value of $\lambda(\tau)$ detectable by our data processing system, i.e., $\lambda(\tau)\approx1$ Hz.

(ii) $\lambda(0)$ may be obtained by fitting Eq. (4.3) with the experimental data. Our determination of $\lambda(0)$ compares fairly closely with the theoretical predictions of Refs. 15–17 derived in the limit of vanishingly small γ and τ:

$$\lambda(0)=\gamma\frac{8\sqrt{2}}{3\pi}\frac{\Delta V}{kT}e^{-\Delta V/kT}. \tag{4.4}$$

The discrepancy with those predictions (some 10–30%) is attributable to finite temperature corrections and increase with $kT/\Delta V$.[16] A detailed analysis of the corrections in γ and kT to $\lambda(0)$ of Eq. (4.4) (Refs. 15 and 16) would require analog simulation at a much lower temperature than feasible with the actual setup of our apparatus.

(iii) κ_0 is proportional to $\Delta V/kT$. Such a dependence is clearly shown in Fig. 6. This means that no more $\lambda(\tau)$ is proportional to the Arrhenius factor $e^{-\Delta V/kT}$ (Refs. 15–17) or, equivalently, that the Arrhenius factor itself is to be modified accordingly.

(iv) κ_0 does not depend on γ. This statement has been verified by varying γ in the regime of interest $\gamma\ll1$.

(v) For a given value of the ratio $\Delta V/kT$, κ_0 is proportional to the potential parameter a. One example of such a dependence is reported in Fig. 6.

The results discussed so far suffice for supporting the claim that colored noise affects the escape process in the underdamped limit through a completely different mechanism than in the overdamped limit. We remember that the τ dependence of $\lambda(\tau)$ in the overdamped limit is closely reproduced by the exponential law

$$\lambda(\tau)=\lambda(0)e^{-\kappa_\infty\tau}, \tag{4.5}$$

where κ_∞ is expressible analytically in terms of the potential and noise parameters.[7] This problem has been investigated in Ref. 10 on employing the continued fraction algorithm of Ref. 2.

A theoretical justification of results (i)–(v) will be given in Sec. VI. Here, we conclude with a final remark. On comparing Figs. 5 and 6 we can easily verify the equality in Eq. (4.2): the smallest Fokker-Planck eigenvalue and the smallest decay rate of $C(t)$ do coincide as expected.

V. SPATIAL RELAXATION IN A MONOSTABLE POTENTIAL

In Sec. III we showed that the relaxation process in the QDW potential can be separated into two distinct mechanisms: the escape over the potential barrier and the re-

laxation inside a single potential well. The former mechanism has been analyzed in detail in Sec. IV. In the present section we focus on the relaxation process in the monostable potential represented by the DO potential (2.3). Such an analysis evidentiates some general features of the librational movement irrespective of the detailed shape of the potential well.

The normalized spatial ACF $C(t)$ of the DO in the underdamped limit exhibits an oscillatory behavior. Its cosine-Fourier transform coincides with the spatial spectral density $S(\omega)$ defined in Sec. III, Eq. (3.3). In Figs. 7 and 8 we display the dependence of $S(\omega)$ on γ and τ, respectively. The main properties of $S(\omega)$ detected through analog simulation may be summarized as follows.

(i) The profile of $S(\omega)$ is smooth and asymmetric. The resonance peak is much steeper on the left-hand side, as predicted in Ref. 19. It must be noted that the theoretical analysis of Ref. 19 refers to the limit of white noise, vanishingly small γ, and weak nonlinearity (low temperature). On the contrary, the experimental data reported in Figs. 7 and 8 have been obtained in a strongly nonlinear regime, i.e., $a=b=0.29\times10^8$ s^{-2} (with x in dimensionless units).

(ii) The resonance peak is enhanced with decreasing γ. This property was also predicted in Ref. 19 for $\tau=0$ and low temperature. With decreasing γ the resonance frequency ω_p shifts to the left approaching $\omega_0+\alpha$ with $\sqrt{\omega_0}=a$ and $\alpha=\frac{3}{4}(b/a)(kT/\omega_0)$.

(iii) The resonance peak is enhanced with increasing τ and shifts to lower frequencies.

Properties (i) and (ii) are explained qualitatively by the theory of Refs. 18 and 19, even if a comparison is out of the question because of the strong nonlinearity simulated in our experiment. Property (iii) instead is rather new and deserves more consideration. In order to provide the reader with quantitative information on the τ dependence of $S(\omega)$ we studied the dependence of the peak frequency $\nu_p(\tau)$ on the noise correlation time τ. Our results are displayed in Fig. 9. $\nu_p(\tau)$ decreases with increasing τ^2 according to a law which is independent of γ, at least to a first approximation ($\gamma\tau\ll1$). $\nu_p(0)$ may be obtained by extrapolating the fitting curve to $\tau=0$ (see also Sec. VI).

We refer the reader to the final section for a theoretical discussion of the results presented in Secs. III–V. Here, it must be noted that in the underdamped limit both $\lambda(\tau)$

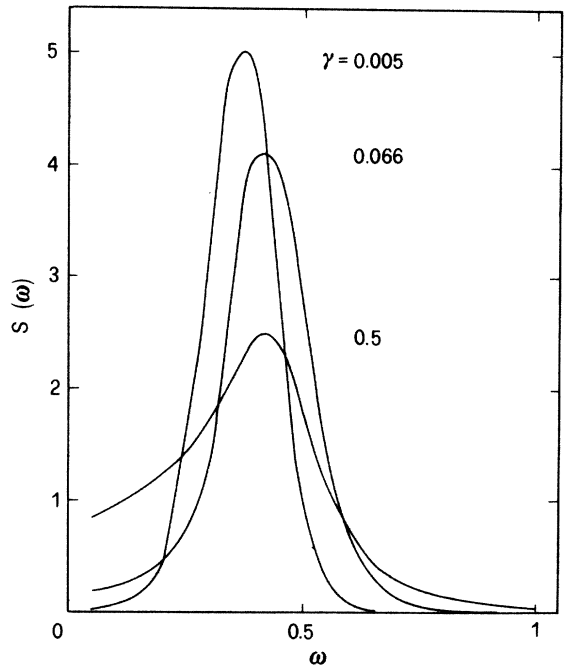

FIG. 7. $S(\omega)$ for the DO potential at different values of γ with $\tau=0.04$ ms. γ and ω are given in units of $\sqrt{a}$.

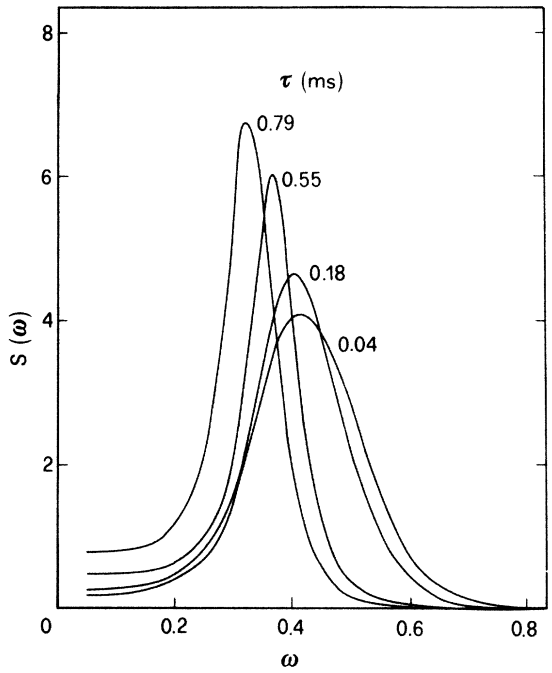

FIG. 8. $S(\omega)$ for the DO potential at different values of τ. $\gamma=0.066\sqrt{a}$, ω is given in units of $\sqrt{a}$.

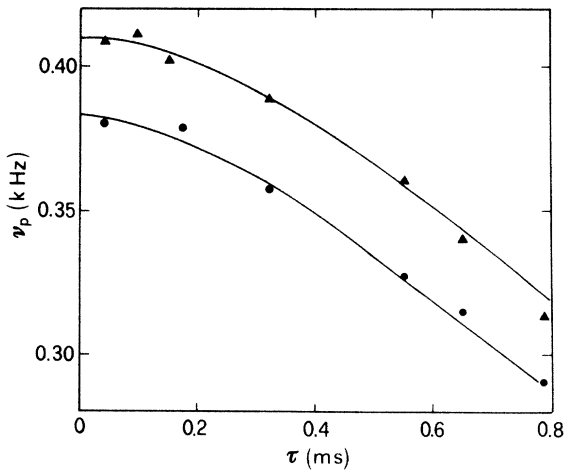

FIG. 9. $\nu_p(\tau)$ vs τ for two values of γ: $\gamma=0.06\sqrt{a}$ (circles) and $\gamma=0.08\sqrt{a}$ (triangles). The solid lines are the corresponding curves of Eq. (6.6).

and $\nu_p(\tau)$ are a function of τ^2. This new behavior is possibly a general feature of the underdamped Brownian motion in the presence of colored noise.

VI. DISCUSSION AND CONCLUSIONS

In the absence of an exhaustive theory for Brownian motion in underdamped potentials driven by colored noise, we limit ourselves to testing the plausibility of our analog-simulation findings and deriving an approximated prediction for $\lambda(\tau)$ and $\nu_p(\tau)$.

Following Kramers's argument[15] for deriving the rate of escape in bistable potentials, we propose to account for the effect of colored noise by renormalizing the ratio $\Delta V/kT$ which appears in Eq. (4.4) for $\lambda(0)$. In the limit of low temperature $kT \ll \Delta V$, the simulation of $C(t)$ for the QDW potential shows that a clear-cut time-scale separation occurs between the spatial relaxation inside the potential wells and the hopping process over the barrier. In the same limit the thermal energy of a bistable oscillator driven by colored noise can be approximated by taking the harmonic expansion of the potential about one of its minima,

$$V(x) \approx (\omega_B^2/2)(x \pm x_\pm)^2 ,$$

with

$$\omega_B^2 = 2a\,(1 - 3kT/8\,\Delta V + \cdots)$$

(Ref. 7). On applying the harmonic analysis expounded in Ref. 24, the cosine-Fourier transform of the spatial ACF of the linearized potential $\hat{C}_L(\omega;\tau)$ can be derived immediately:

$$\hat{C}_L(\omega;\tau) = \frac{1}{\pi} \frac{\hat{C}_\epsilon(\omega)}{(\omega^2 - \omega_B^2)^2 + \gamma^2\omega^2} , \tag{6.1}$$

with $\hat{C}_\epsilon(\omega) = \gamma kT/(1+\omega^2\tau^2)$. After inverse transforming, one arrives at

$$C_L(t;\tau) = \int_{-\infty}^{\infty} C_L(t-s;0) C_\epsilon(s)\,ds . \tag{6.2}$$

In the limit $\gamma \to 0$, $\hat{C}_L(\omega;0)$ is sharply peaked (see Ref. 19 and Sec. V) about $\omega \approx \omega_B$, so that $\hat{C}_L(\omega;\tau)$ can be safely approximated to $\hat{C}_L(\omega;0)/(1+\omega_B^2\tau^2)$. On comparing with Eq. (6.1) we immediately see that such an approximation corresponds to rescaling the equilibrium thermal energy kT of the white-noise source as follows:

$$kT \to \frac{kT}{1+\omega_B^2\tau^2} . \tag{6.3}$$

Operating transformation (6.3) in Eq. (4.4) yields

$$\lambda(\tau) = \lambda(0)(1+\omega_B^2\tau^2)\exp[-(\omega_B\tau)^2\,\Delta V/kT] . \tag{6.4}$$

We recall that our prediction (6.4) is supposedly valid only in the limit $\gamma \to 0$ and $kT \ll \Delta V$. For high potential barriers the correction to the prefactor of $\lambda(0)$ is negligible compared to the Arrhenius factor, ω_B^2 tends to $2a$, and therefore, Eq. (6.4) reduces to the experimental law (4.3) with

$$\kappa_o = 2a\,\Delta V/kT . \tag{6.5}$$

All of properties (i)–(v) of Sec. IV are well reproduced by Eq. (6.5). The quantitative comparison with the experimental results is illustrated in Fig. 10 for one choice of γ. As expected, the best agreement has been obtained for the highest values of $\Delta V/kT$ simulated.

An estimate of $\nu_p(\tau)$ in Sec. V may be obtained as follows. The harmonic approximation introduced above applies to the DO potential, too, with

$$\omega_B = (a/2)\{1 + [1 + 12(b/a^2)kT]^{1/2}\} ,$$

provided that $kT \ll a^2/b$.[19] Under such circumstances the equipartition relation $\omega_B^2\langle x^2\rangle = kT$ with $\omega_B = \omega_p(0)$ holds good at $\tau = 0$. The rescaling (6.3) of the thermal energy in the presence of colored noise may be read as a rescaling of the resonance frequency ν_p, i.e.,

$$\nu_p(\tau) = \frac{\nu_p(0)}{(1+\omega_B^2\tau^2)^{1/2}} . \tag{6.6}$$

The estimate of $\nu_p(\tau)$ in Eq. (6.6) has been reproduced in Fig. 9 for the sake of comparison. The agreement with the results of analog simulation is quite good.

From the discussion of the τ dependence of $\lambda(\tau)$ and $\nu_p(\tau)$ one might conclude that the perturbation corrections due to noise time correlation to the statistical quantities which describe Brownian motion in underdamped potentials are proportional to *even powers of* τ. Such a guess could be confirmed only by a systematic theory of non-Markovian processes.

Finally, we compare our results for $S(\omega)$ in Secs. III and V with the statement of a general theorem proved by Sigeti and Horsthemke.[25] According to such a theorem the spatial density $S(\omega)$ of the system (2.5) should exhibit an ω^{-6} decay for $\omega \gg \gamma, \tau^{-1}$, and ω^{-4} decay for $\gamma \ll \omega \ll \tau^{-1}$, and an ω^{-2} decay for $\omega \ll \gamma, \tau^{-1}$. We were able to verify the above predictions only in the over-

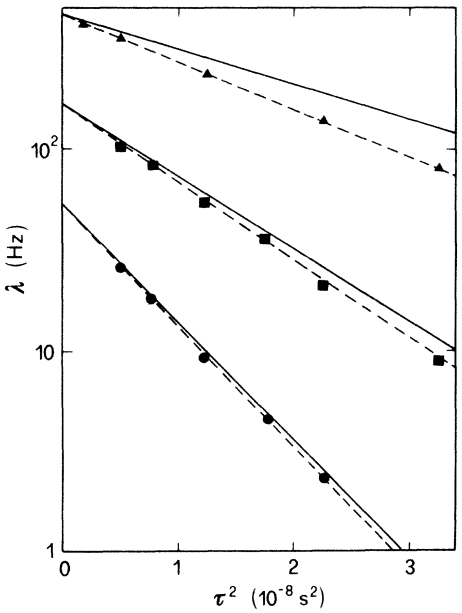

FIG. 10. Comparison of the theoretical prediction (6.4) (solid line) with the experimental data taken from Fig. 6.

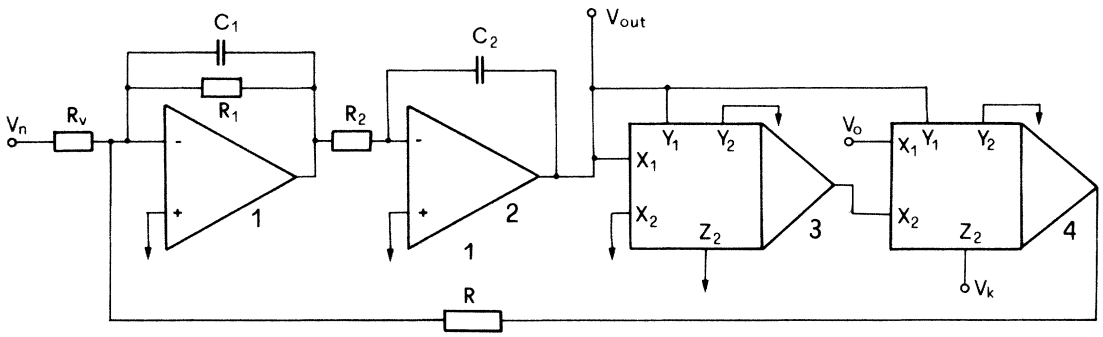

FIG. 11. Block scheme of the analog circuit for the QDW potential.

damped limit $\gamma \ll \omega_p$. In the underdamped limit, instead, we found that $S(\omega)$ falls off faster than any power of ω^{-1}, provided that γ and/or τ^{-1} are taken small enough.

This is no surprise. First of all, we know that in the limit $\tau \to 0$, $\gamma \to 0$, and $kT \to 0$, $S(\omega)$ for the DO potential is approximated by[26]

$$S(\omega)=\begin{cases} \dfrac{\omega-\omega_0}{\alpha}\exp\left[\dfrac{\omega-\omega_0}{\alpha}\right] & \text{for } \omega>\omega_0 \\ 0 \quad \text{for } 0<\omega<\omega_0 \ , \end{cases} \tag{6.7}$$

with $\sqrt{\omega_0}=a$ and $\alpha=\frac{3}{4}(b/a)(kT/\omega_0)$. The analytical expression (6.7) cannot be expanded in a Taylor's series of powers of ω^{-1}. The same argument can be extended to the case of the QDW potential.[26]

Second, in Ref. 25 it is only proved that the coefficients c_n of the ansatz expansion

$$S(\omega)=\sum_{n=0}^{\infty}\frac{c_n}{\omega^{2n}} \tag{6.8}$$

vanish for $n<n_0$. In the case of system (2.5) $n_0=3$. It is well known, however, that series (6.8) is an asymptotic expansion and that in the underdamped case the coefficients c_n may increase further than any power of n—for a review see, e.g., Ref. 27. This implies that the theorem of Ref. 25 is of scarce use in the discussion of our results and, in general, does not provide a hint at a correct modeling of stochastic phenomena.

ACKNOWLEDGMENT

We wish to thank Professor L. Fronzoni for advice and useful discussions.

APPENDIX

The block diagram of the analog circuits used for simulating the QDW and DO potential is displayed in Figs. 11 and 12, respectively. The layout of these electronic circuits is similar to the "minimun-component" scheme of Ref. 12. Blocks 1 and 2 represent two integrators, 3 and 4 are four-quadrant multipliers, and 5 is an inverter amplifier. The operational amplifiers used in 1, 2, and 5 are Op Amp μ741, the two multipliers 3 and 4 are Analog device AD534, the transfer function of which is

$$(X_1-X_2)(Y_1-Y_2)/V_r+Z_2 \ .$$

In our case $V_r=10$ V. The V_0 tension determines the

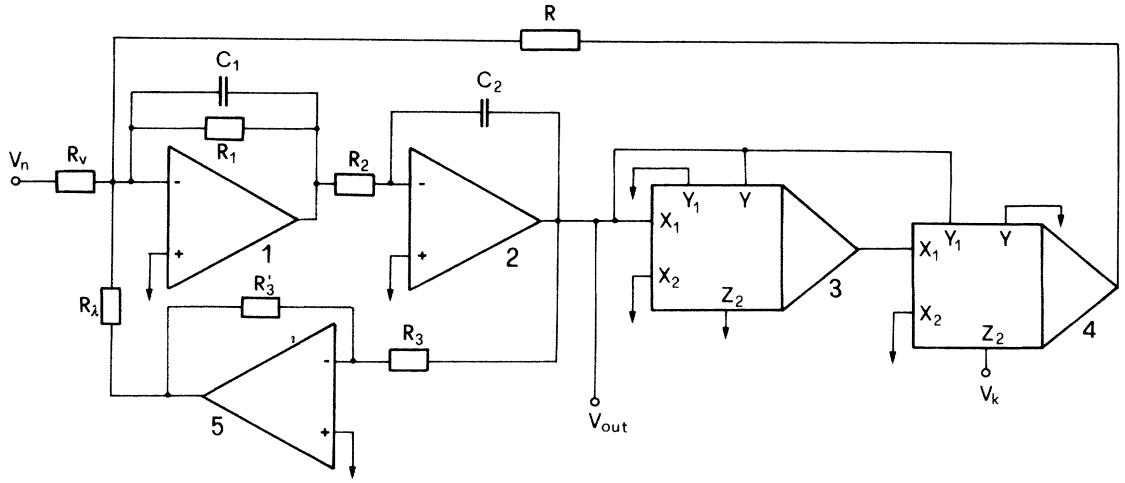

FIG. 12. Block scheme of the analog circuit for the DO potential.

TABLE I. Electronic circuit parameters.

	QDW	DO
$x(t)$	$V_{\text{out}}(t)$	$V_{\text{out}}(t)$
γ	$1/R_1C_1$	$1/R_1C_1$
a	$-V_0/RR_2C_1C_2V_r$	$R_3'/R_3R_\lambda R_2C_1C_2$
b	$1/RR_2C_1C_2V_r^2$	$1/RR_2C_1C_2V_r^2$
$\epsilon(t)$	$V_n(t)/R_vR_2C_1C_2$	$V_n(t)/R_vR_2C_1C_2$

QDW potential shape and was kept constant during the experiment $V_0=4$ V. Note that in circuit of Fig. 11 may be used for simulating the DO potential, too, by simply inverting the sign of V_0. The configuration of Fig. 12, however, is preferred because it allows us to reproduce a wider range of values of the ratio a/b.

The equation simulated by our analog circuits reads

$$\ddot{x}+\gamma\dot{x}+ax+bx^3=\epsilon(t)\ ,$$

where $x(t)$, $\epsilon(t)$, and the parameters γ, a, and b are suitable expressions of the electronic circuit parameters (see Table I).

The setup of our circuit permits us to modify the parameter γ or b/a independently, by varying the resistor R_1 or the tension V_0 (i.e., the resistor R_λ) and leaving the other parameters unchanged.

To compensate for possible asymmetries in the shape of the simulated potential due to offset effects in the multipliers, we applied a very small correction tension V_k (~ 10 mV) to the input Z_2 of the second multiplier. The V_k value was obtained by inspection from the distribution function of the output signal V_{out} and kept constant during the experiment.

The noise signal V_n is obtained by integrating a dichotomic random signal by means of a low-pass filter. The dichotomic signal is produced by feedback on a chain of shift registers[28] with mean-time width of 1.8 μs. The random signal obtained by integration is Gaussian when the time integration constant RC is much larger than the correlation time of the dichotomic signal. In such a case the noise spectral width is given by the reciprocal of the integration constant.

The $x(t)$-signal analysis was performed by means of the Data 6000 waveform analyzer of Analog Data-Precision Division. This instrument acquires, digitizes, and stores analog signals, which are then processed in real time to compute the common statistical quantities like averages, fast Fourier transform (FFT), autocorrelation functions and distributions. As a consequence, high-statistics measurements are obtainable in a relatively short time.

[1] N. G. van Kampen, *Stochastic Processes in Physics and Chemistry* (North-Holland, New York, 1981).

[2] H. Risken, *The Fokker-Planck Equation* (Springer, Berlin, 1984).

[3] R. L. Stratonovich, *Theory of Random Noise* (Gordon and Breach, New York, 1981).

[4] J. M. Sancho, M. San Miguel, S. L. Katz, and J. D. Gunton, Phys. Rev. A **26**, 1589 (1982); K. Lindenberg and B. J. West, Physica A **119**, 485 (1983); L. Masoliver, K. Lindenberg, and B. J. West, Phys. Rev. A **35**, 3086 (1987).

[5] P. Grigolini and F. Marchesoni, Adv. Chem. Phys. **62**, 29 (1985).

[6] P. Hänggi, F. Marchesoni, and P. Grigolini, Z. Phys. B **56**, 333 (1984).

[7] F. Marchesoni, Phys. Lett. **101A**, 11 (1984); Phys. Rev. A **36**, 4050 (1987).

[8] R. F. Fox, Phys. Rev. A **33**, 467 (1986); P. Hänggi, T. J. Mroczkowski, F. Moss, and P. V. E. McClintock, Phys. Rev. A **32**, 695 (1985); J. M. Sancho, F. Sagues, and M. San Miguel, Phys. Rev. A **33**, 3399 (1986).

[9] P. Jung and P. Hänggi, Phys. Rev. A **35**, 4464 (1987).

[10] Th. Leiber, F. Marchesoni, and H. Risken, Phys. Rev. Lett. **59**, 1381 (1987).

[11] F. Marchesoni and P. Grigolini, J. Chem. Phys. **78**, 6287 (1983).

[12] L. Fronzoni, P. Grigolini, P. Hänggi, F. Moss, R. Mannella, and P. E. V. McClintock, Phys. Rev. A **33**, 3320 (1986).

[13] J. E. Straub, M. Borkovec, and B. J. Berne, J. Chem. Phys. **84**, 1788 (1986).

[14] H. A. Kramers, Physica **7**, 284 (1940).

[15] M. Büttiker, P. Harris, and R. Landauer, Phys. Rev. B **28**, 1268 (1983).

[16] H. Risken and K. Voigtlaender, J. Stat. Phys. **41**, 825 (1985); K. Voigtlaender and H. Risken, *ibid.* **40**, 397 (1985); M. I. Dykman, R. Mannella, P. V. E. McClintock, F. Moss, and S. M. Soskin, Phys. Rev. A **37**, 1303 (1988).

[17] V. I. Melnikov and S. V. Meshov, J. Chem. Phys. **85**, 1018 (1986).

[18] W. Renz, Z. Phys. B **59**, 91 (1985).

[19] W. Renz and F. Marchesoni, Phys. Lett. **112A**, 124 (1985).

[20] M. Pochini, S. Santucci, and F. Marchesoni, Z. Phys. B **66**, 243 (1987); F. Marchesoni, M. Pochini, and S. Santucci, *ibid.* **67**, 257 (1987).

[21] P. Hänggi, J. Stat. Phys. **42**, 105 (1986); T. Fonseca, J.A.N.F. Gomes, P. Grigolinin, and F. Marchesoni, Adv. Chem. Phys. **62**, 389 (1985).

[22] T. F. Arecchi and F. Lisi, Phys. Rev. Lett. **49**, 94 (1982).

[23] A first report is contained in F. Marchesoni, E. Menichella-Saetta, M. Pochini, and S. Santucci (unpublished).

[24] R. Kubo, M. Toda, and N. Hashitsume, *Statistical Physica II* (Springer, Berlin, 1985), p. 14.

[25] D. Sigeti and W. Horsthemke, Phys. Rev. A **35**, 2276 (1987).

[26] Y. Onodera, Prog. Theor. Phys. **44**, 1477 (1970).

[27] F. Marchesoni, Z. Phys. B **62**, 505 (1986).

[28] S. Faetti, C. Festa, L. Fronzoni, P. Grigolini, and P. Martano, Phys. Rev. A **30**, 3252 (1984).